Imperfect EM Shielding by Thin Conducting Sheets with PEC and SIBC

M. Leumüller[1], B. Auinger[2], H. Hackl[2], J. Schöberl[1] and K. Hollaus[1]
[1]Technische Universität Wien, Institute for Analysis and Scientific Computing,
A-1040 Vienna, michael.leumueller@tuwien.ac.at
[2]Silicon Austria Labs GmbH, Inffeldgasse 25F, A-8010 Graz

Electromagnetic compatibility of electronic based systems is increasingly gaining importance. The goal is to develop simulation tools, which allow the inclusion of electromagnetic compatibility aspects of electronic based systems. The different dimensions of the involved objects are a big challenge, for example ratios higher than 1:400,000 are common, leading to simplifications like assuming that the shielding is only a boundary condition. The impedance boundary condition is used twice, on the inside and outside of the shielding. A representative example is a small loop antenna located in a metallic box presented here. The antenna is a substitute for more involved emitters.

***Index Terms*—Electromagnetic compatibility EMC, electronic based systems EBS, finite element method FEM, perfect electric conductor, shielding by thin conducting sheets, surface impedance boundary condition SIBC.**

I. Introduction

THE AIM is to develop highly efficient and accurate simulation methods for large complex problems in the context of electronic based systems (EBS) [1]. A big challenge are different dimensions of the involved objects in the simulation of the electromagnetic field, e.g. in cable harnesses [2], [3] or EBS in housings with cut outs [4], [5]. On one hand the source of radiation can be a tiny component on a printed circuit board and on the other the metal housing is comparatively large. Another aspect in this context is the extremely small penetration depths of the electromagnetic field in metallic parts compared to their overall dimensions, which is cumbersome to resolve with the finite element method. Instead the copper traces and the shielding are modeled as boundary conditions. This work is devoted to the second concern.

In particular, a metallic housing is considered once as a perfect electric conductor (PEC) and once with the aid of a surface impedance boundary condition (SIBC) to keep the computational costs small and to still ensure high accuracy. Here, the problem arises how to apply a SIBC simultaneously inside and outside of the housing when it is modeled as a boundary. The simulation domain is split into two. The exterior surrounding and the interior box. The housing surface can be used twice as a boundary condition. The two domains are connected with a penalization on the slot. When the box is modeled as a PEC, the domain doesn't need to be split.

The employed numerical example represents a small loop antenna located in a metallic box with a slot on an infinite metallic plate, see Fig. 1.

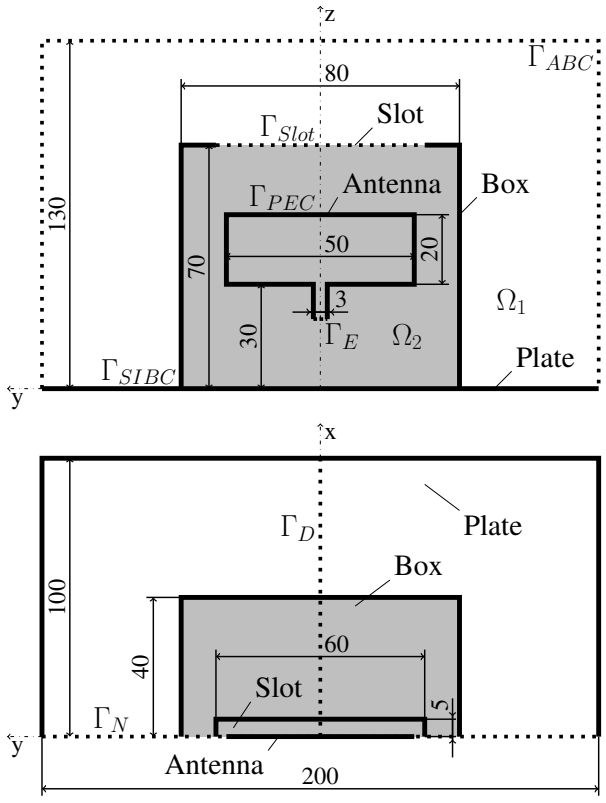

Fig. 1. Geometry of a small loop antenna located in a metallic box with a slot. Cutaway front view (top) and top view (bottom). The cut has been made in the symmetry plane $\Gamma_N(x=0)$. The second symmetry plane is $\Gamma_D(y=0)$. All measurements are given in millimeters (mm). The antenna has a diameter of 1mm.

II. Boundary Value Problem

The boundary value problem to be solved in the frequency domain is based on the magnetic vector potentials $\boldsymbol{A}_1$ with support on the exterior domain Ω_1 and $\boldsymbol{A}_2$ with support in the box Ω_2. They satisfy

$$\begin{aligned} \mathrm{curl}\mu_0^{-1}\mathrm{curl}\boldsymbol{A}_i - \omega^2\epsilon_0\mathbf{A}_i &= \mathbf{0} && \text{in } \Omega = \Omega_1 \cup \Omega_2, \\ \boldsymbol{A}_i \times \boldsymbol{n} &= \mathbf{0} && \text{on } \Gamma_D, \\ \boldsymbol{A}_2 \times \boldsymbol{n} &= \boldsymbol{A}_0 && \text{on } \Gamma_E, \end{aligned}$$

$$
\begin{aligned}
\mu_0^{-1}\mathrm{curl}\boldsymbol{A}_i \times \boldsymbol{n} &= \quad \boldsymbol{0} \quad && \text{on } \Gamma_N, \\
\boldsymbol{A}_i \times \boldsymbol{n} &= \quad \boldsymbol{0} \quad && \text{on } \Gamma_{PEC}, \\
\mu_0^{-1}\mathrm{curl}\boldsymbol{A}_i \times \boldsymbol{n} &= -\tfrac{j\omega}{Z_s}\boldsymbol{A}_{i,t} && \text{on } \Gamma_{SIBC}, \\
\mu_0^{-1}\mathrm{curl}\boldsymbol{A}_i \times \boldsymbol{n} &= -\tfrac{j\omega}{Z_a}\boldsymbol{A}_{i,t} && \text{on } \Gamma_{ABC}, \\
\boldsymbol{A}_{1,t} - \boldsymbol{A}_{2,t} &= \quad \boldsymbol{0} \quad && \text{on } \Gamma_{Slot},
\end{aligned}
$$

where Ω is air, the tangential component $\boldsymbol{A}_{i,t} := \boldsymbol{A}_i \times \boldsymbol{n}$ of $\boldsymbol{A}_i$, the angular frequency $\omega = 2\pi f$, the permeability μ_0 and permittivity ϵ_0. The boundary is divided into the Dirichlet boundary Γ_D arising because of symmetry, the Dirichlet boundary Γ_E for the excitation $\boldsymbol{A}_0$, the Neumann boundary Γ_N again because of symmetry, boundary Γ_{PEC} describing the PEC, the slot Γ_{Slot} connecting the domains and the absorbing boundary Γ_{ABC}. The box Γ_{SIBC} is shared by both domains. Each has its own SIBC on the box. The index $i \in \{1, 2\}$ represents exterior variables and interior variables, see Fig. 1. The antenna is modeled as a PEC. The wave impedance $Z_0 = \sqrt{\frac{\mu_0}{\epsilon_0}}$ is used in the absorbing boundary condition. The SIBC $Z_s = \frac{1+j}{2}\mu_s\omega\delta$ is applied on the box and the metallic plate. The skin depth $\delta = \sqrt{\frac{2}{\omega\mu_s\sigma_s}} \approx 0.205$ µm, permeability μ_s and conductivity σ_s of steel are used. The frequency has been chosen as $f = 3$ GHz. The geometry can be seen in Fig. 1.

III. Weak Form

The weak form is:
Find $(\boldsymbol{A}_1, \boldsymbol{A}_2) \in (V_1, V_2)$ such that

$$
\begin{aligned}
\sum_{i\in\{1,2\}} \Big[\mu_0^{-1} \int_{\Omega_i} \mathrm{curl}\boldsymbol{A}_i \cdot \mathrm{curl}\boldsymbol{v}_i \, dx - \omega^2\epsilon_0 \int_{\Omega_i} \boldsymbol{A}_i \cdot \boldsymbol{v}_i \, dx \\
- \frac{j\omega}{Z_s} \int_{\Gamma_{SIBC}} \boldsymbol{A}_{i,t} \cdot \boldsymbol{v}_{i,t} \, ds\Big] - \frac{j\omega}{Z_0} \int_{\Gamma_{ABC}} \boldsymbol{A}_{1,t} \cdot \boldsymbol{v}_{1,t} \, ds \\
+ \int_{\Gamma_{Slot}} \gamma \left(\boldsymbol{A}_{1,t} - \boldsymbol{A}_{2,t}\right)\left(\boldsymbol{v}_{1,t} - \boldsymbol{v}_{2,t}\right) \, ds = \int_{\Gamma_E} \boldsymbol{A}_0 \cdot \boldsymbol{v}_{2,t} \, ds
\end{aligned}
$$

for all $(\boldsymbol{v}_1, \boldsymbol{v}_2) \in (V_1, V_2)$, with the penalization $\gamma = 10^{10}$ and $V_i := \{\boldsymbol{A}_i \in \mathcal{V}_i : \boldsymbol{A}_i \times \boldsymbol{n} = \boldsymbol{0} \text{ on } \Gamma_D\}$, $\mathcal{V}_i \subset H(\mathrm{curl}, \Omega_i)$ [6]. The boundary integral on Γ_{SIBC} appears in both regions and the boundary integral on Γ_{Slot} enforces the tangential continuity.

IV. Numerical Example

The geometry in Fig. 1 has been used as a numerical example. Because of symmetries, calculations are only carried out on a quarter of the geometry. The interior and exterior B-field with the imposed SIBC can be seen in Fig. 2. The B-fields with imposed PEC boundary condition can be seen in Fig. 3. The fields are shown in a plane parallel to the x-z-plane with a distance of 12mm in y-direction. All simulations were made in the open source finite element software NetGen/NGSolve [7]. The B-field inside the box is stronger than on the outside. For that reason the exterior B-field has been multiplied by a factor of 10.

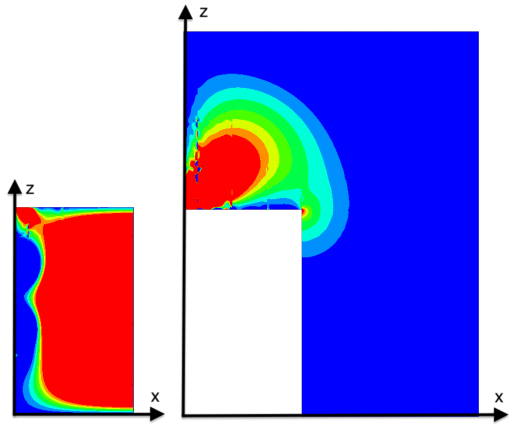

Fig. 2. B-field inside (left) and outside (right) of the box in a plane parallel to the x-z-plane. The real part of the z-component of the B-field is visualized. SIBC is applied on the box and metallic plate. The external field is multiplied by a factor of 10.

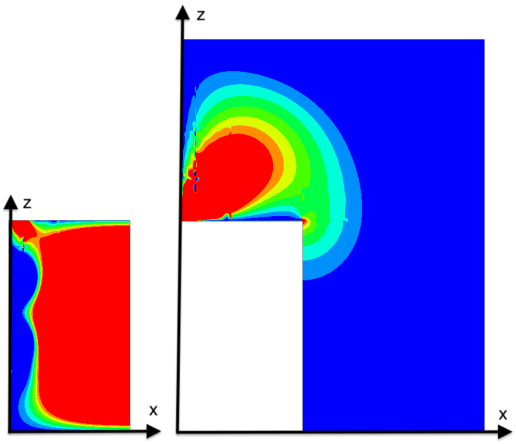

Fig. 3. B-field inside (left) and outside (right) of the box in a plane parallel to the x-z-plane. The real part of the z-component of the B-field is visualized. The box and the metallic plate are modeled as PEC. The external field is multiplied by a factor of 10.

References

[1] K. Hollaus, O. Biro, P. Caldera, G. Matzenauer, G. Paoli, and G. Plieschnegger, "Simulation of crosstalk on printed circuit boards by fdtd, fem, and a circuit model," *IEEE Transactions on Magnetics*, vol. 44, no. 6, pp. 1486–1489, June 2008.

[2] H. Hackl, B. Auinger, B. Deutschmann, and A. Gheonjian, "The shielding effect of a multi-cable harness as function of ic output termination impedance," in *2018 IEEE International Symposium on Electromagnetic Compatibility and 2018 IEEE Asia-Pacific Symposium on Electromagnetic Compatibility (EMC/APEMC)*, May 2018, pp. 707–712.

[3] I. Badzagua, H. Chobanyan, G. Chikovani, I. Oganezova, E. Yavolovskaya, T. Injgia, A. Gheonjian, and R. Jobava, "Effective computational techniques for emc analysis of cable harness," in *2010 XVth International Seminar/Workshop on Direct and Inverse Problems of Electromagnetic and Acoustic Wave Theory (DIPED)*, Sep. 2010, pp. 96–102.

[4] H. Li, "Equipment chassis and housing design for emc," in *2017 IEEE International Symposium on Electromagnetic Compatibility Signal/Power Integrity (EMCSI)*, Aug 2017, pp. 1–17.

[5] S. Iqbal and M. Amin, "An emc retrofit to reduce radiated emission levels in housings/enclosures of space-borne systems," in *2013 IEEE International Conference on Space Science and Communication (IconSpace)*, July 2013, pp. 145–149.

[6] J. Schöberl and S. Zaglmayr, "High order Nédélec elements with local complete sequence properties," *COMPEL*, vol. 24, no. 2, pp. 374–384, 2005.

[7] J. Schöberl. NetGen/NGSolve. [Online]. Available: https://ngsolve.org